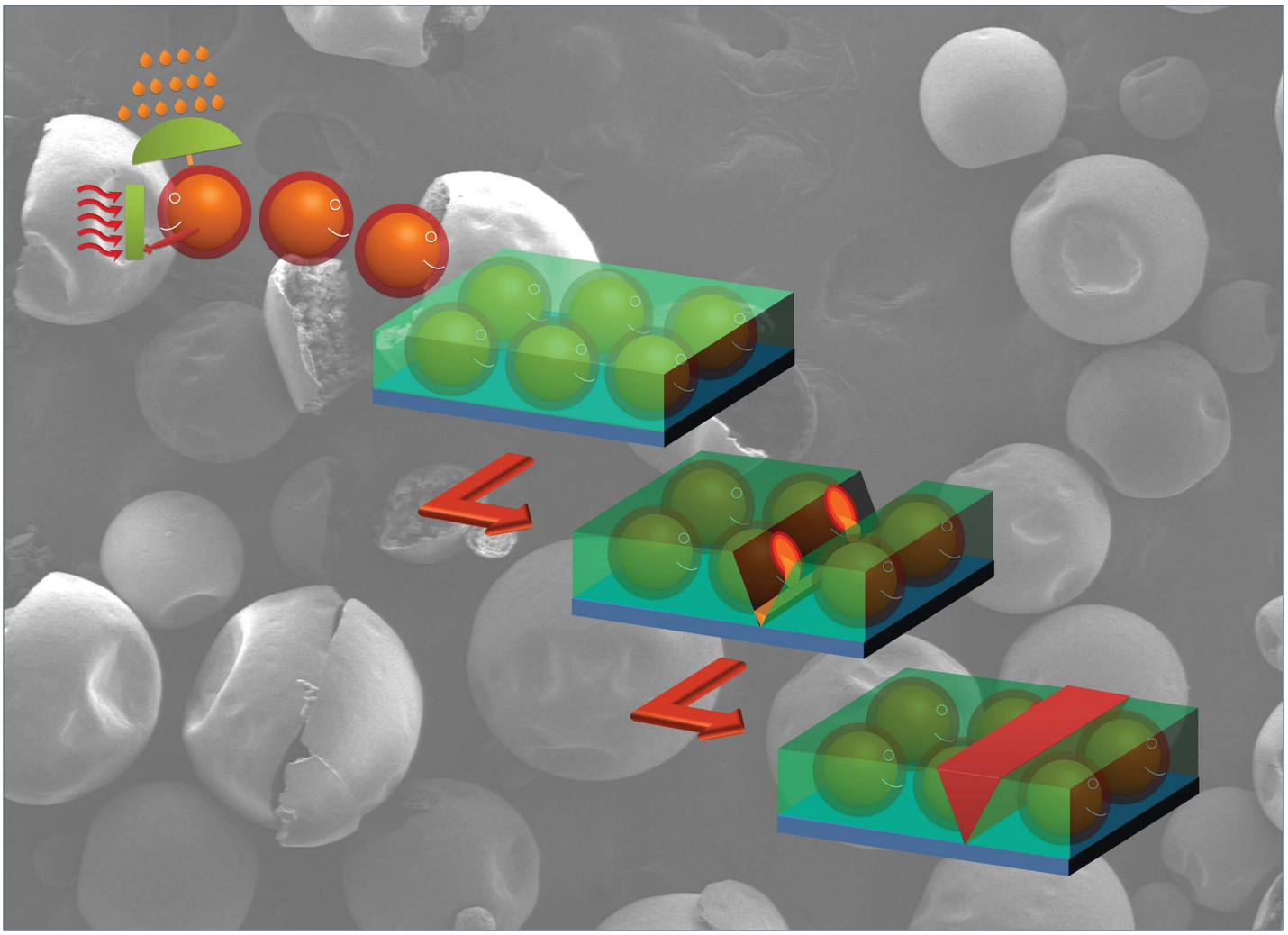

Showcasing research from Dr. Gang Wu and Prof. Yong Xiang, University of Electronic Science and Technology of China, and Prof. Jinglei Yang, Nanyang Technological University, Singapore.

Title: Robust microcapsules with polyurea/silica hybrid shell for one-part self-healing anticorrosion coatings

This work reports novel HDI-filled silica/polyurea hybrid microcapsules, which exhibit superior thermal stability and solvent resistance. The microcapsules were facilely prepared and successfully applied to the one-part self-healing anticorrosion coatings.

As featured in:

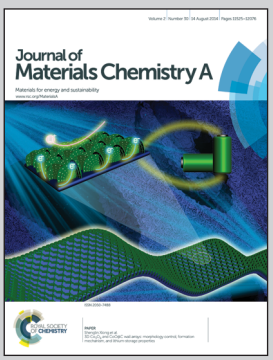

See Yong Xiang, Jinglei Yang *et al.*, *J. Mater. Chem. A*, 2014, **2**, 11614.

ROYAL SOCIETY OF CHEMISTRY

www.rsc.org/MaterialsA

Registered charity number: 207890

Journal of Materials Chemistry A

PAPER

Robust microcapsules with polyurea/silica hybrid shell for one-part self-healing anticorrosion coatings

Cite this: *J. Mater. Chem. A*, 2014, **2**, 11614

Gang Wu,[ab] Jinliang An,[b] Dawei Sun,[b] Xiuzhi Tang,[b] Yong Xiang*[a] and Jinglei Yang*[b]

Silica/polyurea hybrid microcapsules loaded with hexamethylene diisocyanate (HDI) as core materials were prepared *via* a combined strategy of interfacial polymerization and an *in situ* sol–gel process in an oil-in-water emulsion. They were clearly characterized by scanning electron microscopy, Fourier transform infrared spectroscopy, and X-ray photoelectron spectroscopy. The resultant microcapsules have diameters of 57–328 μm, shell thicknesses of 1–8 μm, and core fractions of 51.2–65.6%. The diameter and shell thickness were linearly related to the agitation rate in the double logarithm coordinates, and the core fraction were linearly related to the agitation rate, indicating that the structure and component of the microcapsules can be controlled effectively. The resistant properties against thermal and solvent attacks were assessed by using thermogravimetric analysis and titration. The results show that the microcapsules had outstanding thermal stability with initial evaporation temperature (defined at 5% of weight loss), increased by around 58 °C compared with that of pure core material, and good resistance to xylene with less than 25.9 ± 0.7 wt% reduction of core content after immersion for 100 h. Self-healing anticorrosion coatings based on microcapsules were fabricated on a steel substrate. Preliminary results indicated significant corrosion retardancy occurred in the coatings under an accelerated corrosion process, showing the great potential of our microcapsules in the development of catalyst-free, one-part, self-healing coatings for corrosion control.

Received 17th March 2014
Accepted 14th April 2014

DOI: 10.1039/c4ta01312c

www.rsc.org/MaterialsA

Introduction

The corrosion of materials has attracted attention and concern for a long time as it can lead to considerable economic loss and even endanger human life. For corrosion protection of the surfaces of various substrates, especially metal, coatings mainly consisting of polymer matrix are applied universally. However, cracks in coatings generated from the treating and using of materials can lead to re-exposure of the protected metal substrate in the ambient environment, which results in corrosion.

Microcapsules have been used extensively in many fields, such as biomedical applications,[1,2] catalysis,[3,4] thermal energy storage,[5] and self-healing materials.[6,7] Concerning the self-healing applications of microcapsules, the basic idea is a microcapsules-embedded approach. In other words, microcapsules containing healable agents are embedded into a material's matrix to achieve self-healing of the cracks. Note that the healable agents are usually both flowable and polymerizable. With or without a catalyst, the embedded microcapsules are ruptured as cracks are formed in materials because of mechanical fatigue; moreover, the encapsulated healing agents are released from microcapsules, move into the cracks, form polymers, and finally heal the cracks. The first generation self-healing materials based on this method of embedding microcapsules with a dicyclopentadiene (DCPD) core in the presence of Grubbs' catalyst particles were reported and developed by White *et al.*[6,8–11] Moreover, they also explored the self-healing anticorrosion of epoxy coatings on metal substrates by the microcapsules-embedded approach.[7]

The above-mentioned self-healing materials are typical examples of a so-called two-part self-healing system. The others include multi-part and one-part self-healing systems. Compared with the two-part and multi-part systems, the one-part system could be more promising in practical applications, especially as it minimizes the impact of introducing extra microcapsules to the material matrix, and avoids the use of a catalyst, which is of considerable economic importance. One of a very promising group of candidates available as a one-part catalyst-free self-healing material is microcapsules containing liquid isocyanates, which easily react with moisture. The microcapsules with a polyurethane (PU) shell and isophorone diisocyanate (IPDI) or hexamethylene diisocyanate (HDI) core were obtained by an interfacial polymerization.[12–14] The anticorrosion epoxy coatings

[a]*School of Energy Science and Engineering, University of Electronic Science and Technology of China, Chengdu 610064, China. E-mail: xiang@uestc.edu.cn; Tel: +86-2861831556*

[b]*School of Mechanical and Aerospace Engineering, Nanyang Technological University, Singapore 639798, Singapore. E-mail: mjlyang@ntu.edu.sg; Tel: +65-67906906*

containing the HDI microcapsules were covered on a steel substrate.[13,14] The results indicated that the microcapsules-embedded coatings can heal the cracks from scratches, which significantly avoids corrosion occurring in the cracks of coatings under an accelerated corrosion process.

The one-part microcapsules-embedded approach seems to be preventing the corrosion of materials in real life. However, a universal and critical issue for microcapsules and other micro/nanocontainers is that their resistant property is poor and must be improved for long-term storage and handling in practical applications. The prior strategies of improving the resistant property of microcapsules mainly included preparing multi-layered structured microcapsules,[15–17] introducing inorganic nanosheets into the shell,[18] and increasing the shell thickness;[19] however, their encapsulated substances had relatively high chemical and physical stability. Note that most of the strategies only focused on improving a single resistant property such as thermal resistance, and usually referred to multiple steps. Moreover, the resultant microcapsules might not be of good quality, and some of them were even hard to obtain. Thus, the design and preparation of robust microcapsules with superior resistant properties is quite significant and still extremely challenging for the application of self-healing anticorrosion coatings.

Herein, we present robust microcapsules with a polyurea/silica hybrid shell and HDI core, which were prepared *via* a combined strategy of interfacial polymerization and an *in situ* sol–gel process in an oil-in-water emulsion. The resultant microcapsules showed a significant improvement of thermal and solvent resistant properties. Moreover, the structure and the components of the microcapsules can be controlled effectively. As an example, self-healing anticorrosion coatings are fabricated by dispersing the microcapsules into epoxy coating, which display good corrosion protection performance for steel substrates.

Experimental section

Materials

MDI pre-polymer (Suprasec 2644) was obtained from Huntsman. HDI (99%), gum arabic, tetraethyl orthosilicate (TEOS) (99.9%), polyethylenimine (PEI) (branched, $M_w \sim$ 25 000), ammonium hydroxide solution (28–30%), hydrochloric acid aqueous solution (0.1 mol L^{-1}), bromophenol blue, sodium chloride (NaCl), and anhydrous *p*-xylene (99%) were obtained from Sigma-Aldrich. All chemicals in this study were used without further purification unless otherwise specified.

Preparation of microcapsules with a silica/polyurea hybrid shell and HDI core

A preparation of microcapsules with an HDI core was formed from MDI pre-polymer (Suprasec 2644), branched PEI with 25 000 of Mw, and TEOS. A typical experimental procedure is as follows: at room temperature, 30 mL of 3 wt% gum arabic aqueous solution was prepared as a surfactant solution in a 100 mL beaker. The beaker was suspended in a temperature-controlled water bath on a programmable hot plate with an external temperature probe. The solution was agitated with a digital mixer (Caframo) driving a three-bladed propeller at a rate of 300 rpm and heated to 40 °C with a heating rate of 7 °C min^{-1}. The MDI pre-polymer (0.97 g) was mixed well with HDI (4.8 g), and then this mixture was added into the prepared surfactant solution to develop an emulsion system. After 15 min, the agitation rate and temperature were decreased to 150 rpm and room temperature, respectively. Then, a diluted aqueous solution of 0.1 g of PEI (10 wt%) was added dropwise into the emulsion system to initiate the interfacial polymerization at the oil/water interface. After 30 min, the pre-hydrolyzed product of TEOS (as encapsulation precursor), obtained by mixing and stirring 1 g of TEOS and 2 g of HCl solution (pH = 2.2) at 35 °C for 30 min when the hydrolysis of TEOS was completed, was added dropwise followed by 0.5 g of NH_4OH (28 wt%). The reaction was stopped after 60 min at room temperature, and the resultant microcapsules were washed with deionized water, filtered and air-dried at room temperature for 12 h before further analysis. The amount of dried microcapsules was about 4.5 g.

Morphology and statistic parameters of the HDI microcapsules

The microcapsule formation during the reaction process was observed under an Axiotech optical microscope (Zeiss) equipped with a camera (Sony). The surface morphology and shell thickness were examined using scanning electron microscopy (SEM; JOEL JSM-7600F FESEM). The mean diameter and distribution of the microcapsules were determined from datasets of at least 200 measurements from SEM images and analyzed in Image-Pro Plus 6.0. For SEM observation, the samples were prepared as follows: microcapsules were evenly distributed and mounted on conductive adhesive tape, ruptured with a razor blade to measure shell thickness, and then coated by gold.

Components of microcapsules

The pure HDI, shell and core of microcapsules were analyzed separately by using Fourier transform infrared spectroscopy (FTIR; Varian 3100) in order to confirm the constituents of the microcapsules. The spectrum in the range of 500–4000 cm^{-1} was used for the observation. In order to collect the FTIR spectra of the shell and core, small amounts of microcapsules were crushed and washed 5–7 times by acetone. After filtration and drying, pure core and shells were obtained for analysis, respectively.

Energy-dispersive X-ray spectroscopy (EDX; JOEL JSM-7600F FESEM) was applied to reveal the elemental distribution in the shells of the microcapsules.

X-ray photoelectron spectroscopy (XPS; Axis-ultra, Kratos) was used to detect the chemical composition of the shells. In the XPS experiment, a monochromatized Al Kα X-ray source (1486.71 eV) was operated at a reduced power of 150 W (15 kV and 10 mA). The base pressure in the analysis chamber was

2.66×10^{-7} Pa. The measured binding energies were calibrated by the C 1s (hydrocarbon C–C, C–H) at 285 eV.

Thermal property and core fraction of the microcapsules

The thermal stability property and core fraction of the microcapsules were characterized by using thermogravimetric analysis (TGA; Hi-Res Modulated TGA 2950). The typical experimental procedure is as follows: 10–20 mg of microcapsules was placed in a platinum pan and heated under nitrogen atmosphere at a rate of 10 °C min^{-1} or placed for a certain time at 60 °C in an air atmosphere. The peak width of the derivative of the weight loss curve was used to roughly determine the core fraction of microcapsules.

Solvent resistance

The resistant property of microcapsules with an HDI core in solvent was assessed by the immersion test. Typically, 0.2 g of microcapsules were immersed into 10 g anhydrous *p*-xylene for a certain time at room temperature. Then, 5 g of the upper clear liquid was absorbed and titrated by a standard method of ASTM D2572-97. The relative released percentage of HDI encapsulated in the prepared microcapsules ($HDI_{release}$ wt%) was calculated as follows:

$$HDI_{release}wt\% = \frac{m_{(HDI_{release})}}{m_{(HDI_{encapsulated})}} \times 100\%$$

$$m_{(HDI_{release})} = 2 \times m_{solvent} \times \frac{NCO\%}{1 - NCO\%}$$

$$NCO\% = \frac{(V_{blank} - V) \times C_{(HCl)} \times 0.042}{m_{sample}} \times 100\%$$

where NCO% is the percentage of NCO released into solvent, V_{blank} (mL) is the volume of standard HCl aqueous solution consumed by the blank, V (mL) is the volume of standard HCl aqueous solution consumed by the 5 g specimen, $C_{(HCl)}$ is the normality of standard HCl aqueous solution, 0.042 is the milliequivalent weight of the NCO group, m_{sample} (g) is the weight of specimen (5 g), $m_{(HDI_{release})}$ (g) is the release weight of HDI in total microcapsules, $m_{solvent}$ (g) is the weight of solvent (10 g), and $m_{(HDI_{encapsulated})}$ (g) is the total weight of HDI encapsulated in the initial microcapsules.

Preparation and observation of anticorrosion self-healing coatings

Anticorrosion self-healing coatings were prepared by dispersing 10 wt% of synthesized microcapsules into epoxy resin (EPOLAM 5015) at room temperature, followed by mixing in a hardener (EPOLAM 5015). The mixture was degassed for 20 min under vacuum. A piece of steel plate of 5×5 cm^2 size was polished by sandpaper (grain size 350–400), degreased by acetone, and then washed with distilled water. After being dried, the steel plate was coated by the degassed self-healing coating with about 500–550 μm of thickness. After the epoxy was cured completely at room temperature, scratches were applied manually on the coating by razor blade. Specimens were immersed in 10 wt% of NaCl solution for 48 h to evaluate the accelerated corrosion process. Pure epoxy coating with the same thickness and size was prepared as a control and treated in the same manner for comparison. The corrosion process was recorded by optical photography. The scratched areas were inspected by SEM (JEOL JSM 5600LV SEM) to examine the self-healing performance.

Results and discussion

Preparation and characterization of the microcapsules

As shown in Scheme 1, an oil phase containing Suprasec 2644 and HDI was first dispersed into a gum arabic aqueous solution to generate an oil-in-water emulsion. When PEI was introduced, the primary polymerization reaction between the amino groups of PEI in the aqueous phase and the isocyanate functional group in the oil phase occurred at the oil/water interface to produce a polyurea shell with positive charges surrounding the oil droplets. MDI prepolymer was much more reactive than HDI; thus, the primary reaction was between PEI and prepolymer to form the shell structure, whereas the relatively less reactive HDI liquid was encapsulated as core material. Then, the silica precursors obtained by the pre-hydrolysis of TEOS in hydrochloric acid aqueous solution with pH 2.2 were added dropwise into the emulsion, and were attracted onto the surfaces of the polyurea shell through electrostatic and hydrogen-bonding interactions between amino groups and silanol groups. It is well known that the hydrolysis rate of TEOS is significantly higher than the condensation rate of the silica precursors at around pH 2.0, close to the isoelectric point of silica.[20] The resultant silica precursors, including alkylsilanols and silanols, are water soluble and transparent. As the silica precursors were mixed with emulsion, ammonia water was added dropwise into the reaction system to increase pH values, resulting in an acceleration of the condensation rate of silica precursors; thus, the silica component was successfully hybridized in the polyurea shell by this sol–gel process. In addition, there were some side reactions between NCO groups

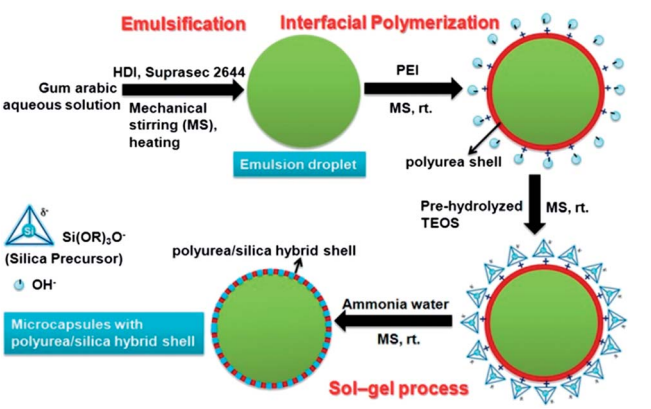

Scheme 1 Preparation of microcapsules with a polyurea/silica hybrid shell and HDI core.

from the prepolymer, intermediate polyisocyanates, HDI and hydroxyl groups from water, and amino groups from NH_4OH. Moreover, these side reactions eventually produced polyurea as a shell wall; however, identifying precisely the chemical compositions of the shell wall material is beyond the scope of this study.

The nearly spherical shaped microcapsules with 328.3 ± 92.9 μm of mean diameter were obtained as shown in Fig. 1a and d. It can be seen that the microcapsules have obvious core–shell structures, and that there are many particles on the outer surface of the capsules (Fig. 1b). Moreover, as shown in Fig. 1c, the shell is quite compact, and the shell wall thickness is roughly uniform and about 8 μm, which acts as an appropriate barrier from leakage and provides enough mechanical stiffness from rupture during post processing.

Using FTIR, the chemical structure of the microcapsules was characterized. As shown in Fig. 2, pure HDI, the capsule shell, and the capsule core were investigated. The nearly identical spectra for HDI and core material indicated that HDI was successfully encapsulated, but no prepolymer was included as can be seen by the absence of signal peaks at 1641.5 cm^{-1} and 1540.7 cm^{-1}.[13] For the shell, the characteristic signal at 1071.2 cm^{-1} is attributed to asymmetric Si–O–Si stretching vibrations of the silica component, and signal peaks at 3311.6 cm^{-1}, 1635.9 cm^{-1}, and 1228.2 cm^{-1} are assigned to hydrogen-bonded N–H stretching vibrations, hydrogen-bonded carbonyl stretching band, and the C–N stretching vibrations of polyurea component, respectively, indicating the silica/polyurea hybrid structure.

Moreover, the presence of the oxygen, nitrogen, carbon, and silicon peaks in the EDX spectrum of the microcapsules' shell reflects the hybrid shell component (Fig. 3a). By XPS of the surface of the microcapsules' shell, oxygen, nitrogen, carbon, and silicon were detected. Fig. 3b depicts the survey spectrum recorded for the microcapsules' shell. The obvious signal peaks of four elements can be observed, as expected. By deconvolving the C 1s and Si 2p peaks (Fig. 3c and d), various components can be obtained. Typically, two components were identified as O=C–NH bonds (288.7 eV) and O–Si (102.8 eV) bonds, which clearly confirms the hybrid shell structure consisting of silica and polyurea.

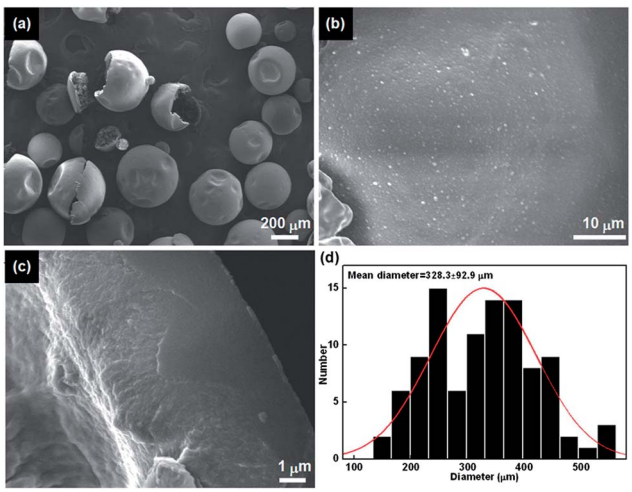

Fig. 1 SEM images of (a) microcapsules, (b) their outer surface, (c) shell wall profile, and (d) histograms of the microcapsules' diameter distribution.

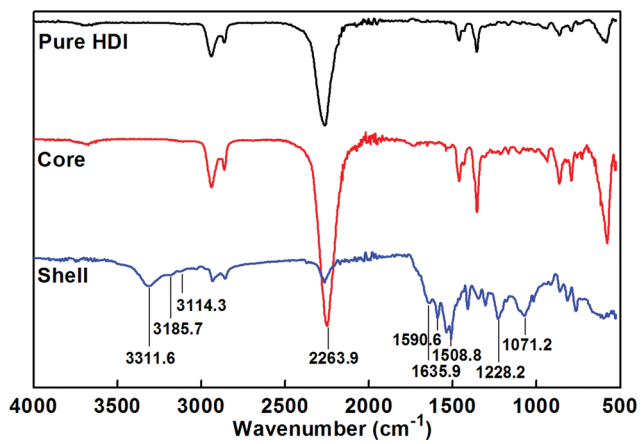

Fig. 2 FTIR spectra of the microcapsules shell, microcapsules core, and pure HDI.

Control of the structure and core fraction of the microcapsules

In the development of microcapsules-based self-healing materials, control of the microcapsule size is a critical issue due to the great influence of diameter on the self-healing performance.[11] Actually, in some cases, only microcapsules with a given range of diameters are suitable. Herein, the average diameter of microcapsules was primarily controlled by the agitation rate. As illustrated in Fig. 4, a higher agitation speed resulted in a smaller microcapsule diameter. The relationship between mean diameter and agitation rate was linear in the double logarithm coordinates, which is consistent with

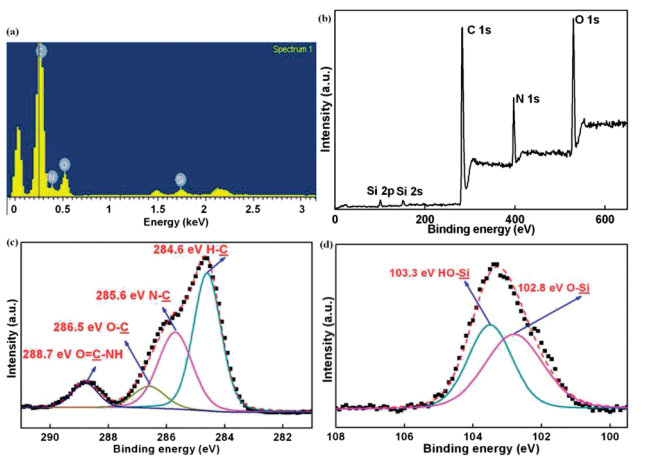

Fig. 3 (a) EDX spectrum of the microcapsules' shell, (b) XPS survey spectrum of microcapsules' shell, and (c) C 1s and (d) Si 2p core line spectra obtained from the microcapsules' shell, respectively. (■) Observed data; (---) theoretical calculated spectra; (—) individual components.

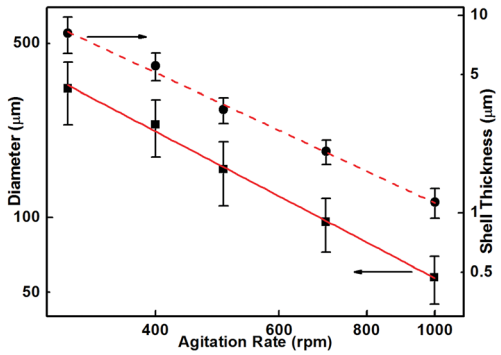

Fig. 4 Diameter and shell thickness of the microcapsules obtained at different agitation rates.

previous reports.[21,22] At higher agitation rates, the stronger shear forces lead to the formation of finer oil droplets in the emulsion system, and the final microcapsules accordingly were of a smaller size. By adjusting the agitation rate from 300 to 1000 rpm, microcapsules with an average diameter in the approximate range of 57–328 μm were obtained.

The influence of the agitation rate on the average shell thickness was also given in Fig. 4, which clearly showed that the shell thickness reduced with increasing agitation rate and their relationship was linear in double logarithm coordinates. As mentioned above, at higher agitation rates, the generated oil droplets were finer, indicating that the total specific surface area of oil droplets was larger. When the amount of core materials was fixed and the shell materials remained constant, the amount of shell materials surrounding each oil droplet would therefore be less, resulting in a thinner shell wall of the resultant microcapsules. By changing the agitation rate from 300 to 1000 rpm, the average shell thickness of microcapsules could be controlled in the range of about 1–8 μm.

Moreover, the core fractions of the microcapsules can also be adjusted through changing the agitation rate. As shown in Fig. 5, faster agitation led to lower core fractions, and the HDI content in the microcapsules reduced from 65.6% to 51.2% with the increase in agitation rate from 300 to 1000 rpm. The reason for this could be that water formation across the thinner capsule shells was easier at higher agitation rates, and accordingly more HDI was consumed by the water. Thus, the core fraction in the final microcapsules was lower at higher agitation rates.

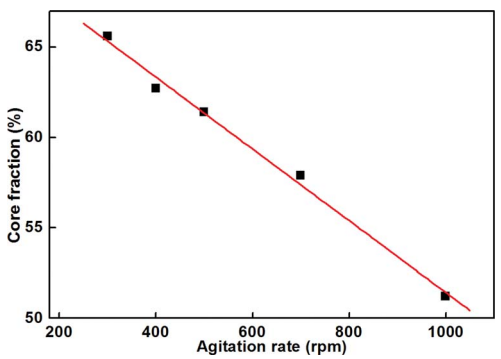

Fig. 5 Core fraction of microcapsules obtained at different agitation rates.

Thermal and solvent resistances of microcapsules

In practical applications, microcapsules have to be robust enough to survive various rigorous environments, such as solvent, moisture, exothermal reaction, acid/base, during the materials' processing cycles.[15,19,23] However, the preparation of robust microcapsules with superior resistant properties, especially regarding solvent and thermal attacks, is still greatly challenging.

As shown in Fig. 6a, the TGA curve shows that the content of HDI in the core was about 65.6%, indicating that the HDI was encapsulated effectively. Remarkably, the initial evaporation temperature (defined at 5% of weight loss) at 144 °C of resultant microcapsules was obviously higher than that of pure HDI (about 86 °C), indicating an excellent thermal resistant property of the microcapsules. In addition, the isothermal experiment of microcapsules in an air atmosphere showed that the residual weights after being heated for 12 h at 60 °C was 86.5% (Fig. 6b), indicating that the thermal stability of HDI in the tight-shell capsules was significantly improved in comparison with that of pure HDI (Fig. 6b). The primary reason for such a tremendous improvement of thermal stability could be the highly cross-linked shell protecting against leakage of the liquid core upon heating.

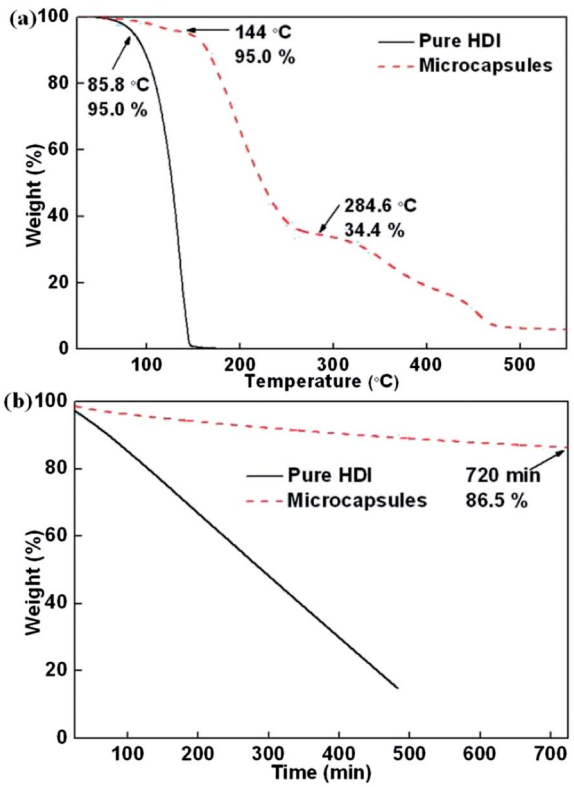

Fig. 6 (a) TGA weight loss curve of the microcapsules and pure HDI with 10 °C min^{-1} heating rate in a N_2 atmosphere, and (b) TGA isothermal curve of the microcapsules and pure HDI at 60 °C in an air atmosphere.

For the application of self-healing anticorrosion coatings, the high resistance of microcapsules to solvents must be highlighted. Since microcapsules emerge in solvents like xylene or toluene, which act as a diluting agent in practical coating systems, the solvent diffuses into the core domain and transfers the core materials out of the microcapsules, which could significantly reduce the self-healing efficiency. Using titration according to ASTM D2572-97, the resistant property of the silica/polyurea hybrid microcapsules in xylene was investigated. It can be seen from Fig. 7 that the relative released percentage of HDI calculated from the titration results gradually reached a plateau after immersion of 100 h, and the final value was 25.9 $\pm$ 0.7 wt%, reflecting a good resistance to xylene as a low polar organic solvent with 2 wt% concentration for a certain period at room temperature.

Corrosion protection assessment of the self-healing coating

Following the procedure described in the above experiment, epoxy coated 5 $\times$ 5 cm^2 steel panels were prepared. After curing in the open air for 24 h, scratches were applied manually on the self-healing coating and the pure epoxy coating as a control by razor blade (Fig. 8a and d). Then, these two specimens were immersed in 10 wt% NaCl aqueous solution at room temperature for 48 h to evaluate the accelerated corrosion process. It can be seen from Fig. 8e that the scratched areas of the self-healing coating were almost completely free of rust after 48 h immersion in salt solution. In contrast, a number of rust areas can be found on the control specimen (Fig. 8b). Indeed, there was no obvious corrosion on the steel panel peeled off the self-healing coating (Fig. 8f), while severe corrosion was apparent on the surface of the steel panel used as a control (Fig. 8c). The results clearly demonstrated the excellent corrosion protection of the prepared self-healing coating towards the steel panel.

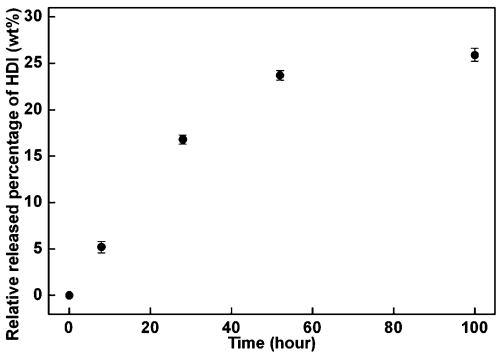

Fig. 7 Relative released percentage of HDI after the microcapsules were immersed in xylene for different times. The concentration of microcapsules was 2 wt%.

The anticorrosion performance was attributed to a self-healing ability of the microcapsules-embedded coating.[13] The difference in the self-healing mechanism from the nanocontainers-based anticorrosion coating[24,25] was that the released HDI from ruptured MCs at scratched areas reacted with moisture or water to form solid materials, which filled the crack. The crack was in this way sealed and healed autonomously, retarding the diffusion of salt ions and thus protecting the substrate from the corrosion process. This mechanism can be supported by SEM observations showing the cracks on the top (Fig. 9a and b) and bottom (Fig. 9c and d) surfaces of the scratched areas of the self-healing coating were filled by newly formed material. The healing process of microcapsules with a silica/polyurea hybrid shell and HDI core in an epoxy coating was completely autonomous, and did not require any catalyst or external intervention. This suggests that this microcapsule can assist in the development of a self-healing anticorrosion coating.

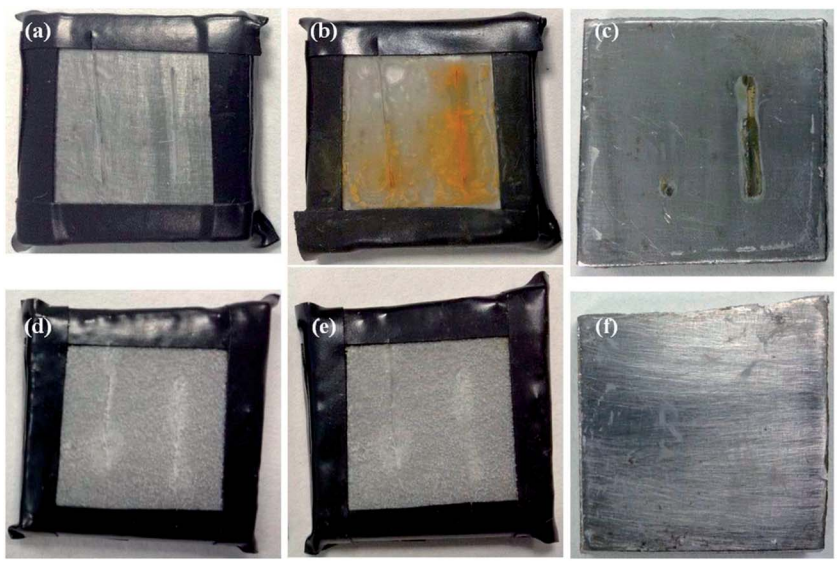

Fig. 8 Corrosion test results for steel panels coated with control and microcapsules-embedded epoxy coating (10 wt% of content of microcapsules), respectively. Control coating: (a) before, (b) after immersion, and (c) steel panel peeled off the coating after immersion. Microcapsules-embedded coating: (d) before, (e) after immersion, and (f) steel panel peeled off the coating after immersion. The panels were immersed in 10 wt % NaCl solution for 48 h.

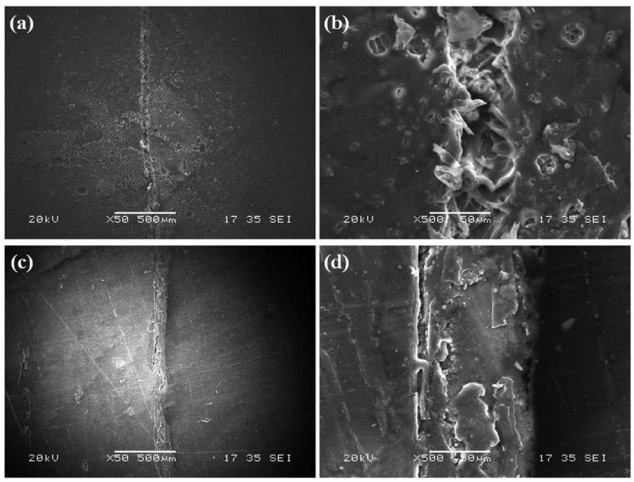

Fig. 9 SEM images of the scratched regions of top (a) and (b), and bottom (c) and (d) surfaces for the self-healing coating after 48 h immersion in salt water.

Conclusions

The spherical silica/polyurea hybrid microcapsules with HDI core were obtained by a combined strategy of interfacial polymerization and an *in situ* sol–gel process in an oil-in-water emulsion. The diameter, shell thickness, and core fraction of the resultant microcapsules can be controlled in the range of 57–328 μm, 1–8 μm, and 51.2–65.6%, respectively. The initial evaporation temperature (144 °C) of HDI (near 5% of weight loss) for silica/polyurea hybrid microcapsules was higher than that of the pure HDI (85.8 °C), and the isothermal experiments at 60 °C in an air atmosphere for 12 h showed that the final residual weight (86.5%) of microcapsules was remarkably higher than that of pure HDI, indicating an outstanding thermal resistant property of our microcapsules. Moreover, after the microcapsules were immersed in xylene with 2 wt% concentration for 100 h, the relative released percentage of HDI was 25.9 ± 0.7 wt%, indicating that the resultant microcapsules had good xylene resistant properties. For the accelerated corrosion process, the scratched areas of the 5 × 5 cm^2 steel panel coated with microcapsules-embedded self-healing coatings were almost completely rust free of rust after 48 h immersion in 10 wt% NaCl aqueous solution at room temperature. In contrast, a number of rust areas could be seen on the control specimen. The result clearly demonstrated the excellent corrosion protection of the self-healing coating towards the steel panel under an accelerated corrosion process, revealing the great potential for the use of our microcapsules in the development of catalyst-free one-part self-healing coatings for corrosion control.

Acknowledgements

J. Yang is grateful to the financial support from the Ministry of Education of Singapore (Tier 1 Grant #: RG17/09) and National Research Foundation of Singapore (Grant #: NRF2011NRF-POC002-044) for this study.

References

1 M. McShane and D. Ritter, *J. Mater. Chem.*, 2010, **20**, 8189–8193.
2 W. Tong, X. Song and C. Gao, *Chem. Soc. Rev.*, 2012, **41**, 6103–6124.
3 S. L. Poe, M. K. lija and D. T. McQuade, *J. Am. Chem. Soc.*, 2007, **129**, 9216–9221.
4 A. R. Longstreet and D. T. McQuade, *Acc. Chem. Res.*, 2013, **46**, 327–338.
5 C. Y. Zhao and G. H. Zhang, *Renewable Sustainable Energy Rev.*, 2011, **15**, 3813–3832.
6 S. R. White, N. R. Sottos, P. H. Geubelle, J. S. Moore, M. R. Kessler, S. R. Sriram, E. N. Brown and S. Viswanathan, *Nature*, 2001, **409**, 794–797.
7 S. H. Cho, S. R. White and P. V. Braun, *Adv. Mater.*, 2009, **21**, 645–649.
8 M. R. Kessler, N. R. Sottos and S. R. White, *Composites, Part A*, 2003, **34**, 743–753.
9 E. N. Brown, S. R. White and N. R. Sottos, *Compos. Sci. Technol.*, 2005, **65**, 2474–2480.
10 J. D. Rule, E. N. Brown, N. R. Sottos, S. R. White and J. S. Moore, *Adv. Mater.*, 2005, **17**, 205–208.
11 J. Rule, N. Sottos and S. White, *Polymer*, 2007, **48**, 3520–3529.
12 J. Yang, M. W. Keller, J. S. Moore, S. R. White and N. R. Sottos, *Macromolecules*, 2008, **41**, 9650–9655.
13 M. Huang and J. Yang, *J. Mater. Chem.*, 2011, **21**, 11123–11130.
14 M. Huang and J. Yang, *Prog. Org. Coat.*, 2014, **77**, 168–175.
15 M. M. Caruso, B. J. Blaiszik, H. Jin, S. R. Schelkopf, D. S. Stradley, N. R. Sottos, S. R. White and J. S. Moore, *ACS Appl. Mater. Interfaces*, 2010, **2**, 1195–1199.
16 Y. Yang, Z. Wei, C. Wang and Z. Tong, *ACS Appl. Mater. Interfaces*, 2013, **5**, 2495–2502.
17 H. Jin, C. L. Mangun, A. S. Griffin, J. S. Moore, N. R. Sottos and S. R. White, *Adv. Mater.*, 2014, **26**, 282–287.
18 C. Fan and X. Zhou, *Polym. Adv. Technol.*, 2009, **20**, 934–939.
19 Q. Li, A. K. Mishra, N. H. Kim, T. Kuila, K. Lau and J. H. Lee, *Composites, Part B*, 2013, **49**, 6–15.
20 H. Zhang, X. Wang and D. Wu, *J. Colloid Interface Sci.*, 2010, **343**, 246–255.
21 E. Brown, M. Kessler, N. Sottos and S. White, *J. Microencapsulation*, 2003, **20**, 719–730.
22 Y.-K. Song and C.-M. Chung, *Polym. Chem.*, 2013, **4**, 4940–4947.
23 D. G. Shchukin, M. Zheludkevich, K. Yasakau, S. Lamaka, M. G. S. Ferreira and H. Möhwald, *Adv. Mater.*, 2006, **18**, 1672–1678.
24 J. J. Fu, T. Chen, M. D. Wang, N. W. Yang, S. N. Li, Y. Wang and X. D. Liu, *ACS Nano*, 2013, **7**, 11397–11408.
25 T. Chen and J. J. Fu, *Nanotechnology*, 2012, **23**, 505750.

